IEEE Access
Multidisciplinary | Rapid Review | Open Access Journal

Received October 27, 2019, accepted November 24, 2019, date of publication December 4, 2019, date of current version January 10, 2020.

Digital Object Identifier 10.1109/ACCESS.2019.2957308

Miniaturized Polarization Insensitive Metamaterial Absorber Applied on EMI Suppression

PANPAN ZUO[1], TIANWU LI[2], MENGJUN WANG[1], HONGXING ZHENG[1], (Senior Member, IEEE), AND ER-PING LI[2]

[1]Key Laboratory of Reliability and Intelligence for Electrical Equipment, School of Electronics and Information Engineering, Hebei University of Technology, Tianjin 300401, China

[2]Key Laboratory of Advanced Micro/Nano Electronic Devices and Smart Systems and Applications, Zhejiang University, Hangzhou 310027, China

Corresponding authors: Hongxing Zheng (hxzheng@hebut.edu.cn) and Er-Ping Li (liep@zju.edu.cn)

This work was supported in part by the National Natural Science Foundation of China under Grant 61571395 and Grant 61671200, in part by the Tianjin Research Program of Application Foundation and Advanced Technology, China, under Grant 14JCQNJC0110, and in part by the Key Project of Hebei Natural Science Foundation under Grant F2017202283.

ABSTRACT This paper presents the analysis and design of a miniaturized polarization insensitive metamaterial absorber (MMA) for suppression of the electromagnetic interference (EMI) at microwave frequency range. The proposed MMA consists of a periodic array of double split ring structures printed on an FR4 substrate with a thickness of 0.07 λ_0. The simulated results derived from CST indicate that the absorption ratio of the MMA is over 90% with a wide frequency range from 8.3 GHz to 11.3 GHz for a normal incident electromagnetic (EM) wave. To understand the EM wave absorption mechanism, an equivalent circuit model of the MMA unit cell is constructed to investigate the absorbing characteristics, and the electric field and surface current distributions are analyzed at absorption peaks.. Both equivalent circuit model (ECM) and measured results show good agreement. What's more, the measurement data shows that the radiated electric field of the patch antenna at 1 meter is significantly reduced at 10 GHz while loading with the MMA. A maximum suppression of 18 dBμV/m is achieved at 10 GHz. As the proposed absorber possesses good ability on electromagnetic radiation absorption, it could be well applied on printed circuit board (PCB) level EMI suppression.

INDEX TERMS Miniaturized, polarization insensitive, metamaterial absorber (MMA), electromagnetic interference (EMI), suppression.

I. INTRODUCTION

Higher data speed leads to faster edge rising rates with more harmonic contents in high-frequency signals, creating more EMI problems [1]. Generally, EMI problems can be tackled in two different ways: one by using a reflective screen and the other by using the absorbers. Though the first solution is the simplest one, it only prevents the EMI in a particular direction by reflecting it but does not minimize the EM pollution, while the second solution can eliminate the EMI by absorbing it completely [2].

MMA is widely applied in real-world applications, like enhancement of electromagnetic compatibility (EMC), EM shielding [3], RCS reduction [4], military radar stealth technology [5]. Many methods have been employed to achieve miniaturized, ultrathin, wideband and polarization-insensitive absorbers. For example, fractal structure [6], [7], resistor-loaded absorber [8], multilayer structure [9]–[11], resistive film [12], [13], magnetic substrate [14], and so on. However, in these previous works, the assembly procedures might be relatively complex and time-consuming, which usually demand careful soldering, precise layer alignments, and high design and fabrication cost [15].

Nowadays, extensive research on MMA is carried out, but a miniaturized, ultrathin and polarization insensitive MMA operating at microwave frequency range with real-world application is still lacking. Therefore, a challenge is to make a state of the art polarization insensitive absorber with ultra-wideband, ultrathin, low cost, light-weight, and excellent shielding ability for EMI reduction applications [2].

In this paper, we design and fabricate the state of the art absorber, which shows perfect absorption above 90% over the

The associate editor coordinating the review of this manuscript and approving it for publication was Nosherwan Shoaib.

frequency range from 8.3 GHz to 11.3 GHz. The proposed MMA can remarkably absorb and reduce the electromagnetic radiation of a patch antenna which works in this absorption frequency band.

The rest of the paper is organized as follows. Section II shows the design and simulation results of the proposed double split-ring absorber (DSRA). In Section III, the equivalent circuit model of the absorber is presented. In Section IV, the experimental result is shown to validate the simulation results, and also, experimental results of assembling the proposed absorber on a patch antenna is presented to verify the EMI suppression performance. Finally, Section V concludes the key findings.

II. DESIGN AND SIMULATION RESULTS

The working principle of absorbers is to match the impedance of the absorber with the free space. This phenomenon, makes the incident waves be absorbed by the designed absorber perfectly. In mathematics, the absorption ratio A is calculated by the formula,

$$A = 1 - S_{11}^2 - S_{21}^2 \tag{1}$$

where S_{11} and S_{21} represent the reflection coefficient and the transmission coefficient, respectively.

As the bottom layer of an absorber is always a continuous metallic ground, so the transmission of electromagnetic waves is blocked. As a result, the transmission coefficient is zero and the absorption ratio A only depends on the reflection coefficient, so the above formula (1) is rewritten as,

$$A = 1 - S_{11}^2 \tag{2}$$

Therefore, by minimizing the reflection coefficient of the MMA, the absorption ability of the structure can be maximized [16].

A. DESIGN OF NOVEL DOUBLE SPLIT-RING ABSORBER

Aiming to obtain the desirable absorption in a wide frequency range centered at 10 GHz, two split concentric rings are utilized to design a double split-ring patch on the top layer, as shown in Fig. 1 (a). The two concentric split rings with different sizes are placed at 90° one to another. Fig.1 (b) shows the cross-sectional view of the absorber. The substrate is made of FR-4 with $\varepsilon_r = 4.4$ and loss tangent $\tan\delta = 0.02$. A continuous metallic film is placed at the bottom layer. The thickness "t" of both the top layer and the bottom layer is 0.035 mm. All the geometrical parameters are listed in Table 1. The MMA unit cell is modeled and simulated using the commercial full-wave simulation software CST STUDIO SUITE.

As shown in Fig. 2 (a), both TE and TM mode absorption performance are coincident, which verifies the polarization insensitive ability of the proposed DSRA. The reflection coefficient S_{11} below −10 dB during the frequency range is from 8.3 GHz to 11.3 GHz. Combined with the results in Fig. 2 (a) with the Equ. (2), the absorption ratio of the proposed DSRA in frequency band from 6 GHz −14 GHz has been calculate, as shown in Fig. 2 (b). The absorption ratio well above 95% is from 8.3 GHz to 11.3 GHz.

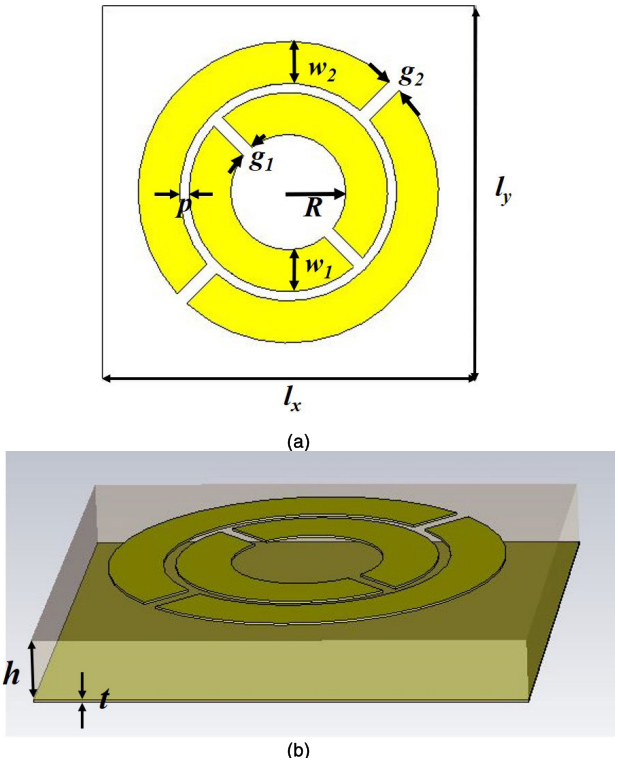

FIGURE 1. Configuration of the proposed double split ring absorber (a) top view (b) side view.

TABLE 1. Geometrical parameters of the DSRA (Unit: mm).

l_x	l_y	R	w_1	w_2
8	8	1.24	0.9	0.9
g_1	g_2	p	h	t
0.25	0.3	0.2	2	0.035

It can be observed from the inset of Fig. 2 (a) that the two resonant frequencies with the values of 9 GHz and 10.3 GHz, respectively, on the reflection coefficient curve, are the absorption peaks in Fig. 2 (b). Moreover, the resonance frequency is determined by the radius of the two rings as shown in Fig. 3 (a) and (b), where it presents with increasing the external ring radius by increasing the value of p, the lower resonant frequency moves to a lower value. Correspondingly, the higher resonant frequency shifts to a higher frequency when the radius of the inner ring R decreases, as shown in Fig. 3 (b).

B. ANALYSIS OF ABSORPTION MECHANISM

The surface current and the electric field distributions on the patch of the proposed DSRA at the resonant frequency, i.e., 9 GHz and 10.3 GHz, are shown in Fig. 4. Fig. 4 (a)-(c) are the current and electric field distributions of the DSRA at 9 GHz, and Fig. 4 (d)-(f) are the current and electric field distributions of the DSRA at 10.3 GHz.

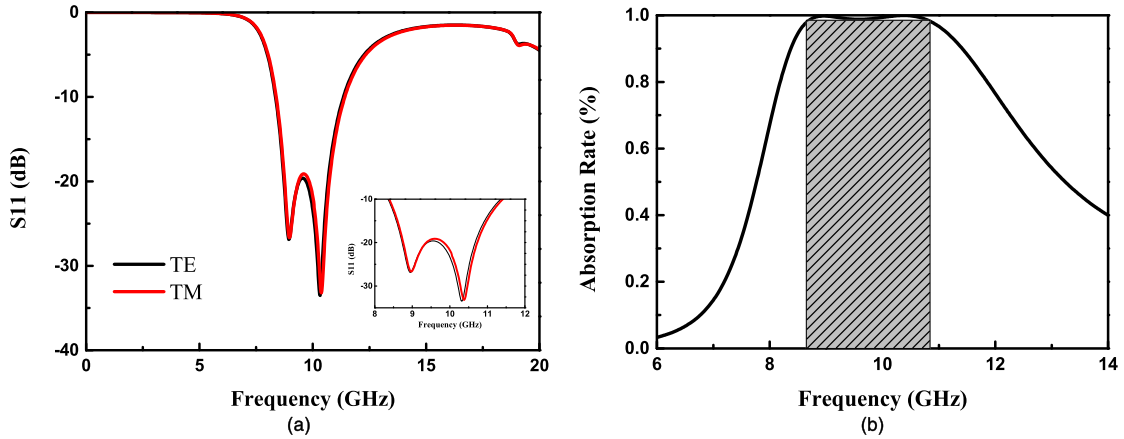

FIGURE 2. Reflection coefficient and absorption rate of the proposed DSRA. (a) TE polarization (solid black) and TM polarization (solid red). (b) absorption rate of the DSRA.

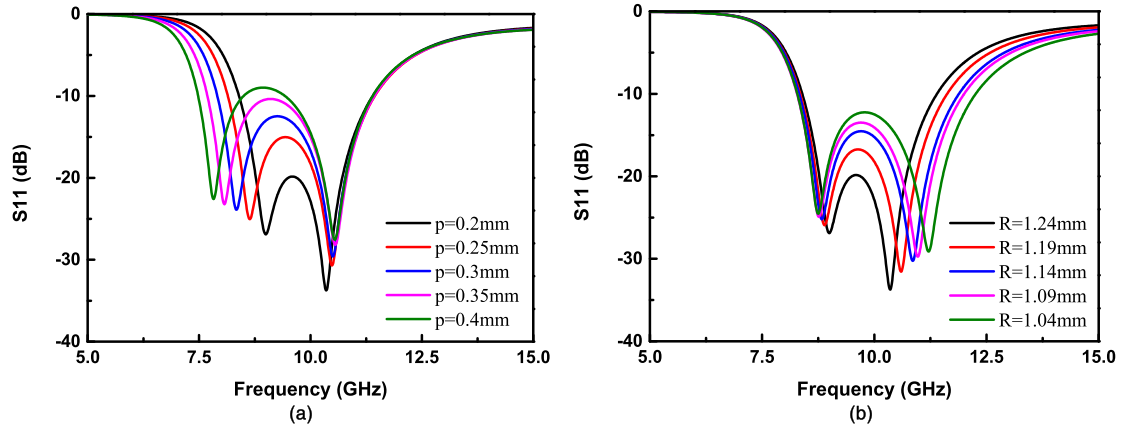

FIGURE 3. Impact of radii on reflection coefficient of the DSRA (a) investigation of lateral radius (b) investigation of inside radius.

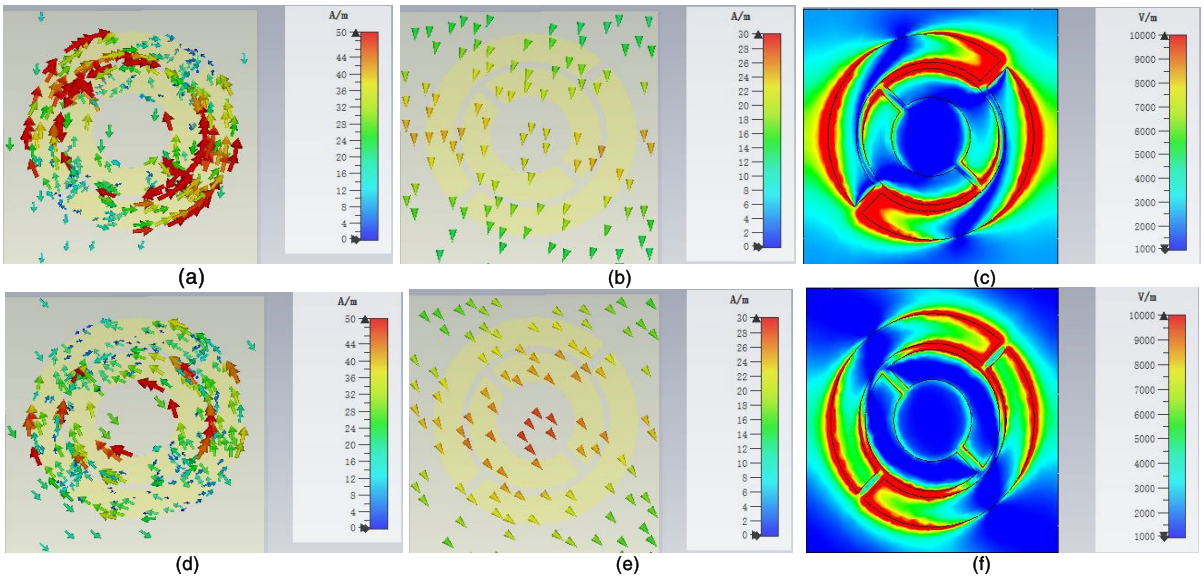

FIGURE 4. Current and electric field distribution of the DSRA (a) current distribution on the patch at 9 GHz (b) current distribution on the ground at 9 GHz (c) electric field distribution on the patch at 9 GHz (d) current distribution on the patch at 10.3 GHz (e) current distribution on the ground at 10.3 GHz (f) electric field distribution on the patch at 10.3 GHz.

As shown in Fig. 4 (a) and (b), the current flowing direction between the top layer and the bottom layer are anti-parallel, so that the induced magnetic resonance manipulates the relative permeability $\mu(\omega)$. Similarly, Fig. 4 (c) indicates that the dielectric constant $\varepsilon(\omega)$ is manipulated by the strong electric field in the capacitive gap on the top layer. When the relative

TABLE 2. Size comparison of the proposed MMA with previous work.

	Techniques	Dimension	Thickness	Absorption ratio
Ref [7]	Fractal structure, resistor-loaded	$0.34\lambda_0$	$0.06\lambda_0$	82%
Ref [18]	Resistor-loaded	$0.45\lambda_0$	$0.5\lambda_0$	90%
Ref [19]	Multilayer structure	$0.41\lambda_0$	$0.2\lambda_0$	90%
Ref [20]	Multilayer structure	$0.621\lambda_0$	$0.1\lambda_0$	80%
Ref [21]	3-D stair-like Jerusalem cross structure	$0.35\lambda_0$	$0.05\lambda_0$	80%
Ref [12]	Resistive film	$0.24\lambda_0$	$0.19\lambda_0$	90%
Ref [17]	Metal-Insulator-Metal (MIM)	$0.43\lambda_0$	$0.1\lambda_0$	83%
Ref [22]	MIM	$0.355\lambda_0$	$0.063\lambda_0$	90%
Ref [23]	MIM	$0.346\lambda_0$	$0.096\lambda_0$	80%
This work	MIM	$0.26\lambda_0$	$0.07\lambda_0$	90%

The dimention and thickness are calculated at the resonant frequency.

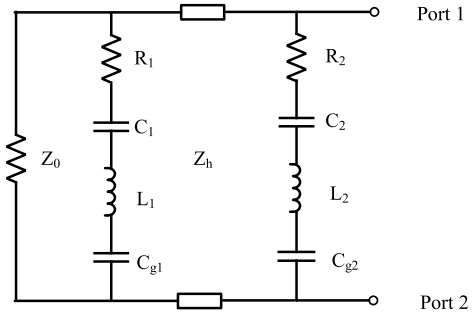

FIGURE 5. Equivalent circuit model of the proposed DSRA.

permeability $\mu(\omega)$ and the dielectric constant $\varepsilon(\omega)$ arrives:

$$Z = \sqrt{\frac{\mu(\omega)}{\varepsilon(\omega)}} = 1 \tag{3}$$

which means impedance match between the absorber and the free space is achieved, the perfect absorption is realized, consequently. Herein, Z is the characteristic impedance of the metamaterial absorber. The perfect absorption corresponding to the perfect impedance matching is obtained when the relative permittivity has the same magnitude with the relative permeability, which is dependent on the coexistence of the strong electric resonance and magnetic resonance [17].

As shown in Table 2, in comparison with the existing metamaterial absorbers, the proposed DSRA is comparatively the most miniaturized and ultrathin under highest absorption ratio.

III. EQUIVALENT CIRCUIT ANALYSIS

The equivalent circuit model of the proposed DSRA is shown in Fig. 5, which consists of two RLC series circuits connected in parallel, representing the two split resonant rings, respectively. Z_h is the equivalent impedance of the lossy grounded dielectric slab. C_{g1} and C_{g2} represent the equivalent capacitances of the splits of the two rings, respectively.

For each ring, the equivalent inductance L is calculated as [24],

$$\frac{L}{Z_0} = \frac{d}{p} F(l, 2w, \lambda) \tag{4}$$

$$F(l, w, \lambda) = \frac{l}{\lambda} \cos\theta [\ln(\cos ec \frac{\pi w}{2l}) + G(l, w, \lambda)] \tag{5}$$

$$G(l, w, \lambda) = \frac{1}{2} \frac{(1-\beta^2)^2[(1-\frac{\beta^2}{4})(A_+ + A_-) + 4\beta^2 A + A_-]}{(1-\frac{\beta^2}{4}) + \beta^2(1+\frac{\beta^2}{2}-\frac{\beta^2}{8})(A_+ + A_-) + 2\beta^6 A_+ A_-} \tag{6}$$

$$A_\pm = \frac{1}{\sqrt{[1 \pm \frac{2l\sin\theta}{\lambda} - (\frac{l\cos\theta}{\lambda})^2]}} - 1 \tag{7}$$

and

$$\beta = \frac{\sin \pi w}{2l} \tag{8}$$

where l and w are the period and width of the DSRA unit cell, respectively. λ is the wavelength. θ is the angle of incidence wave. As the DSRA will be placed very close to the radiation source in practical space extremely limited electronic devices, it is assumed normal incident herein.

The equivalent capacitance C is given as,

$$\frac{C}{Z_0} = 4\frac{\mathrm{d}}{l} F(l, m, \lambda) \tag{9}$$

where m is the pitch between lateral rings of two DSRA unit cells.

For the equivalent circuit of DSRA unit cell, the corresponding equivalent inductance and capacitance parameters are calculated as,

$$\frac{L_{1,2}}{Z_0} = \frac{\mathrm{d}}{l} F(l, 2w, \lambda) \tag{10}$$

$$\frac{C_{1,2}}{Z_0} = 4\frac{\mathrm{d}}{l} F(l, \mathrm{m}, \lambda) \tag{11}$$

TABLE 3. Geometrical parameters of the DSRA (Unit: mm).

R_1	R_2	L_1	L_2
0.0226 Ω	0.015Ω	2.96 nH	2.96 nH
C_1	C_2	C_{g1}	C_{g2}
31.4 pF	26.5 pF	0.105 pF	0.083 pF

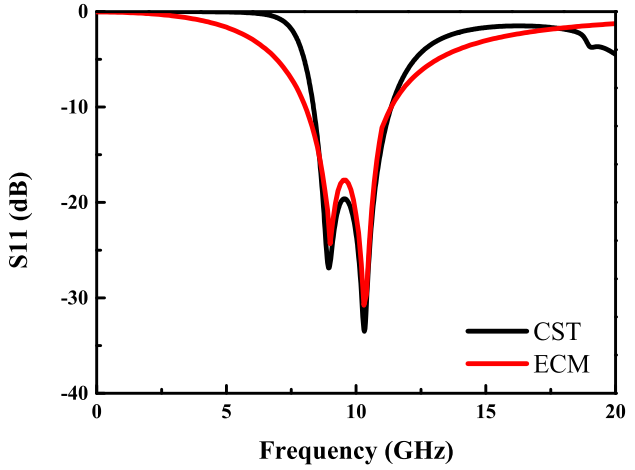

FIGURE 6. Comparison of reflection coefficient obtained by CST and ECM.

$$C_{G1,G2} = \frac{A\varepsilon}{\mathrm{g}} \tag{12}$$

$$R_{1,2} = \frac{\rho \mathrm{l}_r}{A} \tag{13}$$

where A is the cross-sectional area of the split, lr is the length of the ring, ρ is the resistivity of the metal.

The input impedance Z_h of the dielectric slab at normal incidence reads [25],

$$Z_{\mathrm{h}} = j\frac{Z_0}{\sqrt{\varepsilon_r' + j\varepsilon_r''}} \tan(k_0\sqrt{\varepsilon_r' + j\varepsilon_r''}h) \tag{14}$$

where Z_0 is the characteristic impedance of free space, k_0 is the free space propagation constant and h is the thickness of the dielectric substrate. The parameters of the components are summarized in Table 3.

To verify the validity of the equivalent circuit model for the DSRA structure, reflection coefficient obtained by the equivalent circuit model is compared with the simulation results, as shown in Fig. 6.

As shown in Fig. 6, the magnitude of reflection efficiency S_{11} obtained by CST and ECM coordinate well with each other, and both the resonant frequencies and the absorption frequency bands are the same. At 10 GHz, the reflection coefficient of both methods are less than −10 dB, which verifies the correctness and accuracy of the proposed equivalent circuit model.

It is because of the high accuracy and efficiency of the equivalent circuit model that the ECM method is always employed to help predict the absorption band and absorption rate, to provide a good guidance for absorber optimization in packaging design stage.

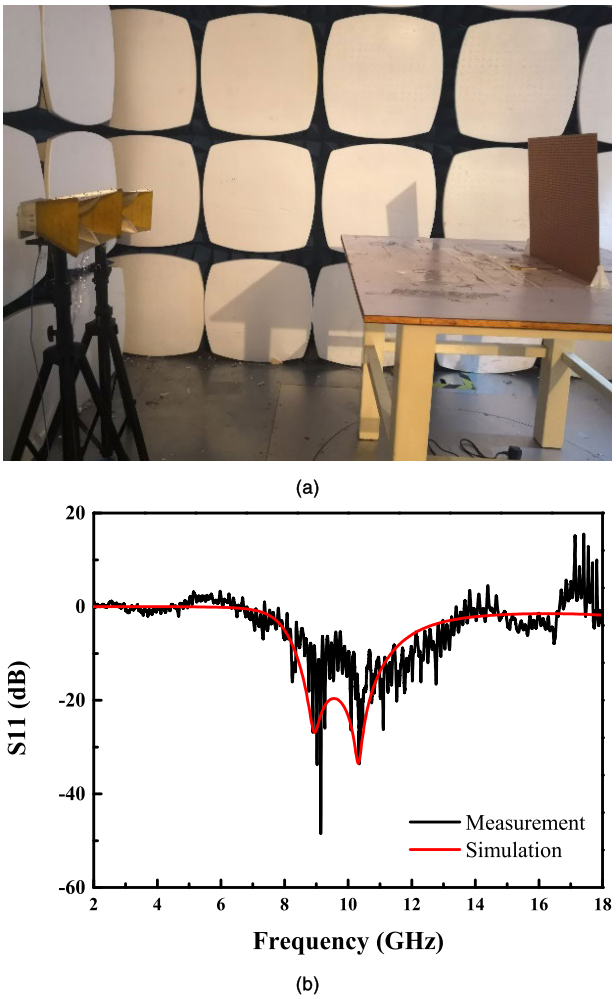

FIGURE 7. Measurement of DSRA (a) photograph of the experiment setup (b) reflection coefficient of DSRA obtained by CST and measurement.

IV. MEASUREMENT RESULTS AND DISCUSSION

A. MEASUREMENT

In order to verify the practical absorption performance of the proposed DSRA, an experiment is carried out in EMC chamber to measure its reflection coefficient.

A 40 × 40 array DSRA sample for test is fabricated, as shown in Fig. 7 (a). The fabricated array sample is put on a wooden desk, with two horn antennas (working in the frequency band 1-18 GHz) facing it. One antenna is used for signal transmitting, and the other for receiving. Both antennas are connected to ROHDE & SCHWARTZ FSW67 signal and spectrum analyzer.

The comparison between the measurement result and the CST simulation result is shown in Fig. 7 (b). It shows excellent agreement with each other, especially at the resonant frequencies, 9 GHz and 10.3 GHz. But due to the unavoidable fabrication and measurement errors, there are some

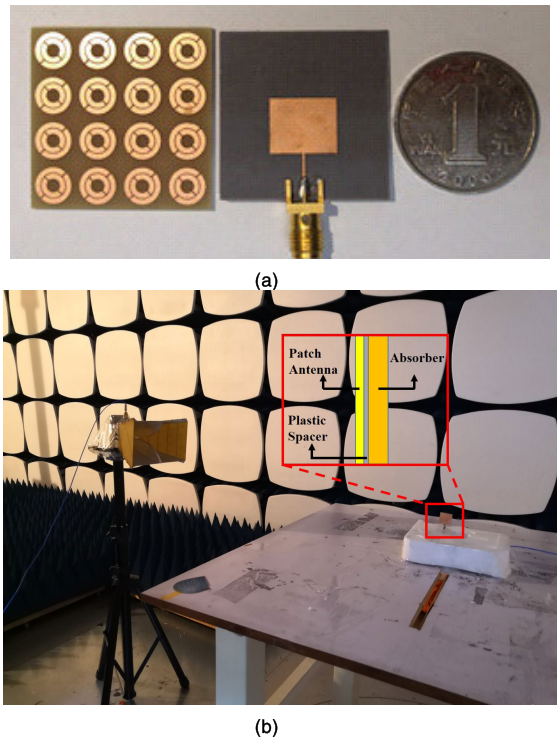

FIGURE 8. EMI suppression application experiment. (a) Photograph of fabricated 4 × 4 DSRA array and the patch antenna. (b) 1 meter radiated electric field measurement setup, inset is the combination and setup of the DUT.

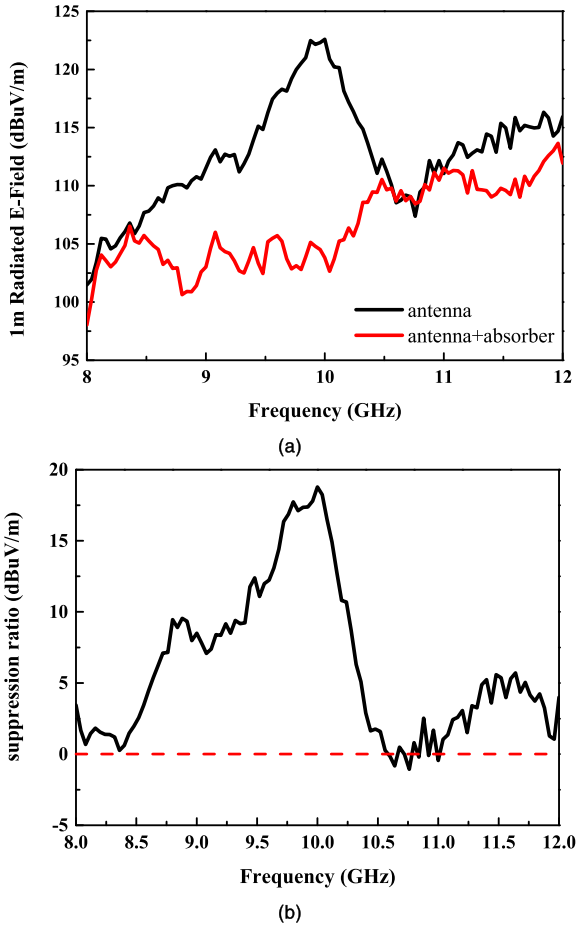

FIGURE 9. Measurement results (a) 1 m radiated E-Field results of the patch antenna w/o the proposed absorber. (b) the suppression ratio of the proposed absorber.

discrepancies on the measurement curve. According to (2), the reflection coefficient curve of the proposed absorber can effectively verify perfect absorption performance.

B. APPLICATION ON EMI SUPPRESSION

For a high speed system, once the EMI source is identified, a suitable volume of absorber material can be placed on the source location to reduce the radiated power at the frequency of interest [26]. In order to verify the EMI suppression ability of the proposed absorber, a 30 mm∗30 mm patch antenna that works at 10 GHz is fabricated to generate the radiation source, and a 4 × 4 DSRA array is utilized for EMI suppression. The photograph of the established experiment is shown in Fig. 8 (a).

The patch antenna is excited by Keysight E8267D Signal Generator over the frequency band that ranges from 8 GHz to 12 GHz through a SMA-type connector, driving the antenna to generate electromagnetic radiation, and the input power is 20 dBm. In the measurement, a plastic spacer with a thickness of 0.2 mm is inserted to separate the patch antenna and the absorber, as shown in the inset of Fig. 8 (b).

As shown in Fig. 8 (b), a horn antenna that captures the radiated electric field works as the receiver in the measurement. It is located 1 m distant horizontally from the radiation source. The measured radiation emission is sent back to an Agilent Signal and Spectrum Analyzer N9020A.

To record the maximum electromagnetic radiation, the antenna is set both in TE and TM polarization, and the wooden desk is rotated by 360°. The height of the horn antenna is changed over the range from 0.8 m to 1.6 m.

The measured 1 m electromagnetic radiation is processed to be the radiated electric field.

$$E(\frac{dB\mu V}{m}) = 107 + U(dBm) + L(dB) + A_F(\frac{dB}{m}) \quad (15)$$

where E is the received electric field, U is the measured radiation power on the spectrum analyzer, L is the loss of coaxial cables, and A_F is the antenna factor.

Fig. 9 (a) shows the measured at 1 m radiated electric field results of the patch antenna w/o the proposed absorber in the EMC chamber. Obviously, the case with the absorber has much lower radiation than the antenna radiation. As shown in Fig. 9 (b), at the antenna working frequency, the radiated electric field is suppressed 18 dBμV/m, which implies that in advanced package, the undesirable radiation could be effectively suppressed if the proposed absorber is in use.

V. CONCLUSION

A miniaturized, ultra-thin and polarization insensitive metamaterial absorber consisting of double split-rings is proposed in this paper. The MMA structure achieves a perfect absorption ratio during a wide frequency range of 8.3 GHz - 11.3 GHz. The surface current and electric field distributions of the proposed MMA unit cell are analyzed to further understand the absorption mechanism. The designed structure is fabricated and tested. The measured results show that with the proposed MMA, the undesired electromagnetic radiation is significantly suppressed at a maximum value of 18 dBμV/m at the designed frequency. The experiment validates the effective EMI absorption and suppression ability of the proposed MMA design, and proves that the proposed DSRA is practical in EMI suppression applications.

REFERENCES

[1] E. Bogatin, *Signal and Power Integrity—Simplified*. Upper Saddle River, NJ, USA: Prentice-Hall, 2010.

[2] M. M. Tirkey and N. Gupta, "Electromagnetic absorber design challenges," *IEEE Electromagn. Compat. Mag.*, vol. 8, no. 1, pp. 59–65, 1st Quart., 2019.

[3] Y. Murata, T. Kanamoto, and F. Murase, "Wideband shield door with a magnetic absorber," *IEEE Trans. Electromagn. Compat.*, vol. 55, no. 3, pp. 526–531, Jun. 2013.

[4] P. Mei, X. Q. Lin, J. W. Yu, A. Boukarkar, P. C. Zhang, and Z. Q. Yang, "Development of a low radar cross section antenna with band–notched absorber," *IEEE Trans. Antennas Propagat.*, vol. 66, no. 2, pp. 582–589, Feb. 2018.

[5] D. Wu, Y. Liu, Z. Yu, L. Chen, R. Ma, Y. Li, R. Li, and H. Ye, "Wide-angle, polarization-insensitive and broadband absorber based on eight-fold symmetric SRRs metamaterial," *Opt. Commun.*, vol. 380, pp. 221–226, Dec. 2016.

[6] N. I. Landy, S. Sajuyigbe, J. J. Mock, D. R. Smith, and W. J. Padilla, "Perfect metamaterial absorber," *Phys. Rev. Lett.*, vol. 100, May 2008, Art. no. 207402.

[7] L.-L. Liu, H.-F. Zhang, and L.-L. Wang, "A novel broadband metamaterial absorber based on the fractal structure," in *Proc. Progr. Electromagn. Res. Symp. (PIERS)*, Aug. 2016, pp. 1928–1931.

[8] Y. Shang, Z. Shen, and S. Xiao, "On the design of single–layer circuit analog absorber using double-square-loop array," *IEEE Trans. Antennas Propagat.*, vol. 61, no. 12, pp. 6022–6029, Dec. 2013.

[9] H. Xiong, J.-S. Hong, C.-M. Luo, and L.-L. Zhong, "An ultrathin and broadband metamaterial absorber using multi-layer structures," *J. Appl. Phys.*, vol. 114, no. 6, Aug. 2013, Art. no. 064109.

[10] F. Ding, Y. Cui, X. Ge, Y. Jin, and S. He, "Ultra-broadband microwave metamaterial absorber," *Appl. Phys. Lett.*, vol. 100, no. 10, Art. no. 103506, Mar. 2012.

[11] P. Zhong, X. Hou, and Q. Zhang, "An optimized ultrathin and broadband metamaterial absorber using slotted square loop with multi layers," in *Proc. Int. Conf. Microw. Millim. Wave Technol. (ICMMT)*, May 2018, pp. 1–3..

[12] H. B. Zhang, P. H. Zhou, L. W. Deng, J. L. Xie, D. F. Liang, and L. J. Deng, "Frequency-dispersive resistance of high impedance surface absorber with trapezoid-coupling pattern," *J. Appl. Phys.*, vol. 112, no. 1, Jul. 2012, Art. no. 014106.

[13] Y. Pang, H. Cheng, Y. Zhou, and J. Wang, "Analysis and enhancement of the bandwidth of ultrathin absorbers based on high-impedance surfaces," *J. Phys. D, Appl. Phys.*, vol. 45, no. 21, May 2012, Art. no. 215104.

[14] R. Huang and Z.-W. Li, "Broadband and ultrathin screen with magnetic substrate for microwave reflectivity reduction," *Appl. Phys. Lett.*, vol. 101, no. 15, Oct. 2012, Art. no. 154101.

[15] Z. Zhou, K. Chen, B. Zhu, J. Zhao, Y. Feng, and Y. Li, "Ultra–wideband microwave absorption by design and optimization of metasurface salisbury screen," *IEEE Access*, vol. 6, pp. 26843–26853, 2018.

[16] S. Bhattacharyya, S. Ghosh, D. Chaurasiya, and K. V. Srivastava, "A broadband wide angle metamaterial absorber for defense applications," in *Proc. IEEE Int. Microw. RF Conf. (IMaRC)*, Dec. 2014, pp. 33–36.

[17] W. Xin, Z. Binzhen, W. Wanjun, W. Junlin, and D. Junping, "Design and characterization of an ultrabroadband metamaterial microwave absorber," *IEEE Photon. J.*, vol. 9, no. 3, pp. 1–13, Jun. 2017.

[18] J. Zhao and Y. Cheng, "Ultrabroadband microwave metamaterial absorber based on electric SRR loaded with lumped resistors," *J. Electron. Mater.*, vol. 45, no. 10, pp. 5033–5039, Oct. 2016.

[19] X. Qiu, Y.-C. Jiao, L. Zhang, and Y. Chang, "Ultra-broadband metamaterial absorber with resistances loaded," in *Proc. 6th Asia–Pacific Conf. Antennas Propag. (APCAP)*, Oct. 2017, pp. 1–3.

[20] S. Bhattacharyya, S. Ghosh, D. Chaurasiya, and K. V. Srivastava, "Bandwidth-enhanced dual-band dual-layer polarization-independent ultra-thin metamaterial absorber," *Appl. Phys. A, Solids Surf.*, vol. 118, no. 1, pp. 207–215, Jan. 2015.

[21] D. Lim, S. Yu, and S. Lim, "Miniaturized metamaterial absorber using three–dimensional printed stair–like jerusalem cross," *IEEE Access*, vol. 6, pp. 43654–43659, 2018.

[22] B.-Y. Wang, S.-B. Liu, B.-R. Bian, Z.-W. Mao, X.-C. Liu, B. Ma, and L. Chen, "A novel ultrathin and broadband microwave metamaterial absorber," *J. Appl. Phys.*, vol. 116, no. 9, Sep. 2014, Art. no. 094504.

[23] S. Ghosh, S. Bhattacharyya, and K. V. Srivastava, "Bandwidth-enhancement of an ultrathin polarization insensitive metamaterial absorber," *Microw. Opt. Technol. Lett.*, vol. 56, no. 2, pp. 350–355, Feb. 2014.

[24] R. Langley and E. Parker, "Equivalent circuit model for arrays of square loops," *Electron. Lett.*, vol. 18, no. 7, p. 294, 1982.

[25] F. Costa, S. Genovesi, A. Monorchio, and G. Manara, "A circuit–based model for the interpretation of perfect metamaterial absorbers," *IEEE Trans. Antennas Propag.*, vol. 61, no. 3, pp. 1201–1209, Mar. 2013.

[26] Q. Liu, X. Jiao, J. Li, V. Khilkevich, J. Drewniak, P. Dixon, and Y. Arien, "Modeling absorbing materials for EMI mitigation," in *Proc. IEEE Int. Symp. Electromagn. Compat. (EMC)*, Aug. 2015, pp. 1548–1552.

PANPAN ZUO was born in Tai'an, China, in 1988. She received the B.S. degree in electrical engineering from Inner Mongolia University, Hohhot, China, in 2010. She is currently pursuing the Ph.D. degree in electrical engineering with the Hebei University of Technology, Tianjin, China.

Her current research interests include electrical modeling and design of 3-D electronic packages, signal integrity, and power integrity in high-speed packages.

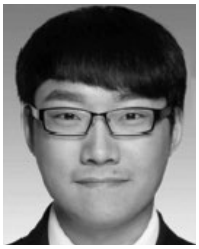

TIANWU LI received the B.S. degree in communication engineering from Shandong University, Weihai, China, in 2016. He is currently pursuing the M.S. degree in electronic engineering with Zhejiang University, Hangzhou, China.

His current research interests include frequency selective surface and the radome and antenna of 5G communication technology.

MENGJUN WANG received the B.S. degree in information engineering and the M.S. degree in physical electronics from the Hebei University of Technology, Tianjin, China, in 1999 and 2005, respectively, and the Ph.D. degree from Tianjin University, Tianjin, in 2008.

He is currently an Associate Professor with the School of Electronics and Information Engineering, Hebei University of Technology. His research interests include microwave radio frequency technology, flexible electronics devices, and electromagnetic compatibility.

HONGXING ZHENG was born in Yinchuan, Ningxia Hui Autonomous Region, China. He received the B.S. degree in physics from Shaanxi Normal University, Xi'an, Shaanxi, China, in 1985, and the M.S. degree in physics and the Ph.D. degree in electronic engineering from Xidian University, Xi'an, in 1993 and 2002, respectively.

From 1985 to 1989 and 1993 to 1998, he was a Lecturer with the Ningxia Institute of Technology, Yinchuan, Ningxia, China. From 2001 to 2002 and 2004 to 2005, he was a Research Assistant and a Research Fellow with the Department of Electronic Engineering, City University of Hong Kong, Kowloon, Hong Kong, respectively. In 2003, he was a Postdoctoral Research Fellow with the College of Precision Instrument and Opto-Electronics Engineering, Tianjin University. He is currently a Professor with the School of Electronics and Information Engineering, Hebei University of Technology, Tianjin, China. He has authored six books and book chapters and more than 80 journal articles and 50 conference papers. His recent research interests include modeling of microwave circuit and antenna and computational electromagnetics.

Dr. Zheng is a Senior Member of the Chinese Institute of Electronics. He received the University Distinguished Teacher Award of the Tianjin University of Technology and Education, in 2012, and the 2008 Young Scientists awards presented by the Tianjin Municipality, China.

ER-PING LI received the Ph.D. degree in electrical engineering from Sheffield Hallam University, Sheffield, U.K., in 1992.

From 1989 to 1992, he was a Research Associate/Fellow with the School of Electronic and Information Technology, Sheffield Hallam University. From 1993 to 1999, he was a Senior Research Fellow, the Principal Research Engineer, and the Technical Director of the Singapore Research Institute and Industry, Singapore. Since 2000, he has been serving to the Singapore National Research Institute of High Performance Computing, Singapore, as the Director of the Advanced Electronic Systems and Electromagnetics Department, and the Senior Director for the Collaborative Research. Since 2010, he has been with Zhejiang University, Hangzhou, China, where he is currently a Changjiang–Qianren Distinguished Professor with the Radio Frequency and Nano electronic Research and the Dean of Zhejiang University/University of Illinois at Urbana–Champaign Institute. He has published more than 400 articles in the refereed international journals and conferences, and authored two books published by Wiley/IEEE Press and Cambridge University Press. His research interests include fast and efficient computational electromagnetics, microscale/nanoscale integrated circuits and electronic package, EMC, SI, and nanotechnology.

Dr. Li is a Fellow of the Electromagnetics Academy, USA. He was an elected the IEEE EMC Distinguished Lecturer, from 2007 to 2008. He received numerous awards, including the IEEE EMC Technical Achievement Award and the IEEE Richard Stoddard Award in EMC. He is also an Associate Editor of the IEEE TRANSACTIONS ON COMPONENTS, PACKAGING, AND MANUFACTURING TECHNOLOGY and the IEEE TRANSACTIONS ON ELECTROMAGNETIC COMPATIBILITY. He was the President of the International Zurich Symposium on EMC, Singapore, in 2006 and 2008, the General Chair for the 2008, 2010, and 2012 Asia-Pacific International EMC Symposium, and the Chairman of the IEEE EMC Singapore Chapter, from 2005 to 2006. He has been an invited Speaker for numerous talks and keynote speeches at various international conferences and forums.